J Mater Sci: Mater Med (2008) 19:1515–1522
DOI 10.1007/s10856-008-3385-6

ESEM evaluations of muscle/nanoparticles interface in a rat model

Antonietta M. Gatti · James Kirkpatrick · Andrea Gambarelli · Federico Capitani · Torsten Hansen · Rosy Eloy · Gaelle Clermont

Received: 8 November 2007 / Accepted: 9 January 2008 / Published online: 12 February 2008

Abstract In order to examine the influence that shape and chemistry of different materials have on the incitement of a tissue reaction, we implanted five materials (the two metals Ni and Co, the two ceramics TiO_2 and SiO_2, and the polymer poly vinyl-chloride) as nanoparticles or bulk, in the dorsal muscles of 50 rats. After 6 or 12 months, rats were euthanized and the implanted materials were excised together with the surrounding tissue. After a first histological evaluation, the specimens were prepared for environmental scanning electron microscopy (ESEM) and for energy dispersive spectroscopy (EDS), in order to analyse the chemical composition of the implanted material after the biological interaction had occurred, and to evaluate the possible corrosion and diffusion of the materials at tissue interface. The results indicate that the metals at nanoscale size have a carcinogenic effect, while the bulk materials only induce a foreign-body reaction. The ESEM observations show a chemical transformation of the materials. Corrosion of the metals and subsequent recombination of the released ions in a sort of organic–inorganic crystals is showed and verified by the EDS analyses. Finally, our hypotheses of the involved pathological mechanism are suggested.

A. M. Gatti (✉) · A. Gambarelli · F. Capitani
Laboratory of Biomaterials, Department of Neurosciences, Head and Neck, Rehabilitation, University of Modena & Reggio Emilia, Via Campi 213/A, 41100 Modena, Italy
e-mail: antonietta.gatti@unimore.it

J. Kirkpatrick · T. Hansen
Institute of Pathology, J. Gutenberg University, Mainz, Germany

R. Eloy · G. Clermont
Biomatech, Chasse-sur-Rhone, France

1 Introduction

Nanotechnology is an emergent area of research because of the very special properties that materials at nanoscale level show. These new aspects induced industry to invest an impressive amount of money in order to develop products, instruments and new methodologies exploiting those properties. Novel applications of nanotechnologies can be found, among many others, in the fields of medicine (nanomedicine), of food (nanofood), of biotechnologies. Products that contain nanoparticles (NPs) are already present on the market (such as toothpaste, toothbrushes, antibacterial T-shirts, golf balls, etc.) and most people use nanotechnological products everyday, probably without being conscious of it. Several recent studies have pointed out the need to investigate the impact of these new technologies on human health [1–3]. It fact, the biocompatibility of most NPs has never been verified, both for economic interest and for the lack of suitable tests.

It has been demonstrated that inhaled nanoscale-size particulate matter can trigger lung pathologies [4, 5]. Breathing of asbestos fibres, that are technically nanofibres since at least one of their dimensions is at nanoscale level, has been related to pleural mesothelioma. Silicosis is caused by inhalation of silica particles, which are suspected to traslocate and disseminate to other organs [6–8]. Also the wear debris released by internal hip-joint prostheses is known to induce a local granulomatosis and, because of the nanoscale size, can migrate to other organs like the liver, the kidneys, the spleen and the lungs [9, 10]. Once there, they accumulate and can promote further diseases [11–14].

Other studies verified the presence of micro- and nano-pollution in some pathological tissues affected by cancer or diseases of unknown origin [15]. The concern of possible side effects of these NPs on humans and animals is

increasing, so it is important to verify if NPs induce different effects from the bulk material of the same chemical composition [16, 17].

The European Project Nanopathology (QOL-2002–147) investigated the in vitro [18, 19] and in vivo reactions of NPs and bulk materials in order to show if the shape and size of particles can induce different reactions, in vivo.

Aim of this work is the analysis of five different materials in a bulk and nanoscale shape after implantation in rats, and the evaluation of their local and systemic effect by means of environmental scanning electron microscopy (ESEM) and an energy dispersive spectroscopy (EDS).

2 Materials and methods

2.1 Nanoparticles

Five different materials were selected for the in vivo test: two metals: cobalt (Co) (Sigma Chemicals, Germany) and nickel (Ni) (University of Bologna, Italy), two ceramic materials: titania (TiO_2) and silica (SiO_2) (TAL Materials Inc., USA) and one polymer: poly vinyl-chloride (PVC) (European Vinyl Corporation Int., UK). They were selected considering their chemical and physical properties especially in relation to their biocompatibility. Ni and Co are metals which can corrode and release metallic ions. TiO_2 and SiO_2 are ceramic materials and are chemically inert. Finally, PVC is a polymer, synthesized without additives which are considered toxic like phthalates. Bulk materials were shaped as discs with a diameter of 6–12 mm and a height of 2 mm, while the NPs (see Table 1) had the following sizes: Co = 50–200 nm, Ni = 50 nm; PVC = 60–170 nm, TiO_2 = 20–160 nm; SiO_2= 4–40 nm. The NPs were observed by means of an ESEM (FEI QUANTA; the Netherlands) equipped with an EDS (EDAX, USA) and transmission electron microscopy (TEM) (JEOL 2010, Japan). Figure 1 shows the NPs under ESEM (a), TEM (b) and the surfaces of the bulk materials (c). Figure 2 shows the disc and the NPs of cobalt under ESEM.

SiO_2 and TiO_2 particles were produced using a patented flame spray pyrolysis process involving combusting aerosols of single-metal and mixed-metal metallo-organic alcohol solutions, with oxygen or air in a reaction chamber at temperatures of 1,200–2,000°C. Rapid quenching produces essentially unagglomerated, single particle, nanopowders with the same composition as in the original precursor solutions. PVC NPs were obtained from a microsuspension of an emulsion of PVC (EC DIRECTIVE 91/155 EEC). Ni NPs were developed starting from power of Ni 99.9% of 3–7 μm size. A 2-h crushing in a shaker-mill (SPEX 8000) in controlled (Argon) atmosphere produced non-agglomerated crystallites (Table 2).

2.2 Rats experiments

The different NPs were solubilized and 1 ml of each suspension was withdrawn in a sterile syringe and weighted. The singular weights are reported in Table 2. Then, NPs and bulk materials were sterilized in ethylene oxide gas. Fifty-five Sprague–Dawley male rats, about 3-weeks old (IFFA Credo, France), were divided into five groups of ten animals for the experiments, and five rats were used as controls. The animals were implanted bilaterally with the same material in their back: subcutaneously with bulk material and intramuscularly with NPs. The rats were anaesthetized by intramuscular injection of Tiletamine-Zolazepam (dose of 50 mg/kg body weight). An incision large enough to accommodate the sample was made in one side of the back through the skin and parallel to the vertebral column. A pocket was formed by blunt dissection in the subcutaneous tissue in which the implant material was introduced. The bulk material was implanted on the right

Table 1 List of properties of NPs

Sample	Particle size (diameter)	Compositional mapping	Ultrastructure
TiO_2	Average = 70 nm Range ~20–160 nm	Titanium, oxygen	Grain boundaries
SiO_2	Average = 15 nm Range ~4–40 nm (smaller particles) Range ~100–400 nm (larger particles)	Silicon, oxygen	Amorphous
PVC	Average = 130 nm Range = 60–170 nm	Carbon, chlorine	Necks connecting particles
Cobalt	Range ~50–200 nm	Cobalt, oxygen, iron	Crystalline
Nickel	Average = 140 mm Range = 40–420 mm	Nickel, oxygen	Crystalline

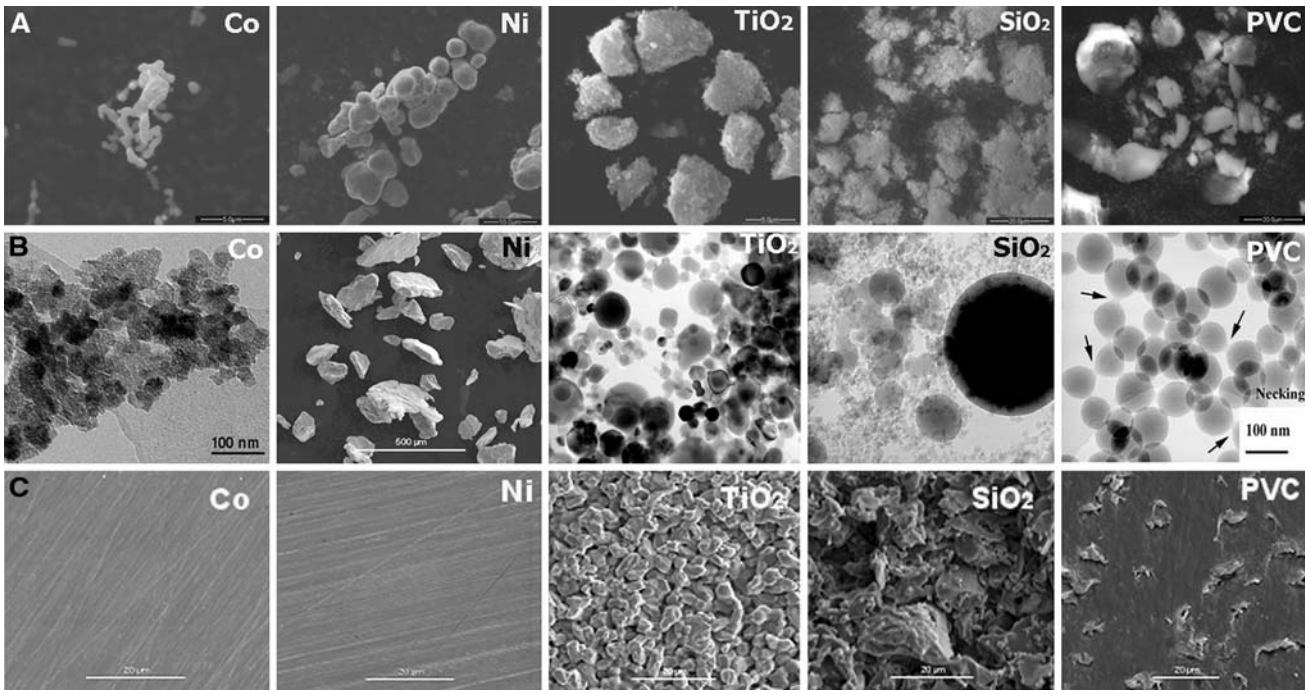

Fig. 1 Images of NPs of cobalt, nickel, titania, silica and PVC, under ESEM (**a**), TEM (**b**) and ESEM images of the bulk material surfaces (**c**)

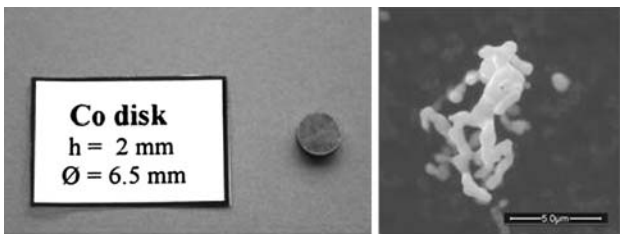

Fig. 2 Images of the cobalt disk and NPs

side of the vertebral column of each animal, and on the left side, in the paravertebral muscle, the NP material were pushed.

The animal tests were performed in compliance with the local ethics committee and husbandry was carried out following the European standard requirements for all the times of the experiment: 6 and 12 months. The animals were observed daily and anomalies such as changes in skin and fur, respiratory, circulatory, autonomic and central nervous systems were reported, as well as behaviour pattern changes in comparison to the control group.

2.3 Environmental scanning electron microscopy

At the deadline of the experiments, each animal was euthanized by injection of a sodium pentobarbital-based drug and local macroscopic features such as necrosis, exudates, haemorrhage, fibrous tissue, etc., were reported. The tissue surrounding the site of implantation was excised, fixed in 4% PBS-buffered formalin and prepared for the electron scanning microscopic examinations.

After a dehydration in ascending concentrations of alcohols, the samples were embedded in paraffin and sectioned with a microtome in 10-μm thick sections. They were deposited on acetate sheets and after a treatment with xylol drops to eliminate the paraffin, they were placed on an adhesive carbon disc, on an aluminium stub, and inserted in the chamber of the ESEM. This miscroscope was coupled to EDS to characterize the morphology of the NPs, bulk discs and the surrounding tissue.

No coating of an electro-conductive layer on the sample surface was carried out, since the instrument used allows the observation of the actual morphology of organic and

Table 2 List of the weights (g) of NPs for every syringe

NPs	Syringe A	Syringe B	Syringe C	Syringe D	Syringe E	Syringe F	Syringe G	Syringe H	Syringe I	Syringe L	Average
TiO2	0.0272	0.0198	0.0214	0.0226	0.0263	0.0235	0.0205	0.0256	0.0178	0.0288	0.02335
SiO2	0.0048	0.004	0.0037	0.0063	0.0049	0.0051	0.0072	0.0056	0.0055	0.0056	0.00527
Co	0.1047	0.0817	0.0957	0.0797	0.0903	0.0861	0.1058	0.0661	0.0705	0.0719	0.08525
PVC	0.0566	0.0507	0.0536	0.0582	0.0618	0.0582	0.0585	0.0618	0.0602	0.0605	0.05801
Ni	0.1028	0.0855	0.1167	0.0819	0.0751	0.1005	0.1038	0.1251	0.1113	0.0251	0.09278

inorganic matter without any treatment, contamination or alteration.

3 Results

The ESEM observations verified that all the NPs were agglomerated. Especially Ni formed microsize particles and they were not examined by TEM. This clustering is due to the propensity of NPs to agglomerate, and it must be taken into account when considering the interaction with tissue. The in vivo tests, scheduled at 6 and 12 months, were interrupted prematurely at 8 months for the rats that were treated with Ni- and Co NPs. In fact, these rats developed a rare form of cancer of the soft tissues: rhabdomyosarcoma. The other materials did not induce lethal reactions, but only inflammation, granuloma or fibrotic capsule formation. The details of the histo-pathological results are reported in an article by Hansen et al. [20].

Figure 3 shows the images of the dorsal back of rats after 6-month subcutaneous and muscular implantation of silica and titania bulk materials. No necrosis or particularly serious inflammation is visible. The ESEM observations of the implanted material and of the surrounding tissue reveal interesting aspects that will be considered material by material.

Ni as NP and bulk material induced rhabdomyosarcoma just after 6 month post-implantation, so the animals were euthanized before the scheduled time. The ultramicroscopic images of the implantation area showed the formation of new calcium–phosphate agglomerates, absent in the back of control-group rats. Figure 4b shows a wide calcified area: its peculiarity is that this calcification is composed by single particles, spherically shaped, ranging 2–10 μm. The wide calcified area rises from the coalescence of the single spheres. This calcification seems to start directly from the material (Ni particles). Figure 4a shows debris surrounded by the tissue; the relevant chemical spectrum contains not only Ni but also C and P.

Fig. 3 Macrophotograph of the subcutaneous and intramuscular implantation of titania (**a**) and silica (**b**) in bulk and nanoscale shape

So, while Ni induced neoplasia both as implanted bulk material and NPs, the Co discs developed inflammation and granuloma at 6 months and preneoplasia at 12 months. The Co NPs, instead, at 6 months induced preneoplastic lesions that turned into sarcoma at 12 months (Fig. 5).

The ESEM analyses carried out in the area where the NPs were inserted showed the formations of new Co crystals (Fig. 6) and Co–P aggregates around the NPs. On the bulk sample site, there was the formation of Ca–P aggregates with Fe around the Co disc.

The SiO_2 discs and NPs showed an inflammatory reaction, but it was not possible to find the relevant NPs. Figure 7 shows the site where they were located, now replaced by Ca and P.

The TiO_2 disc induced only inflammation while the NPs-induced granuloma. Figure 8 shows areas of NP agglomeration embedded in a reactive tissue. The EDS signal issued by the particles includes also other ions (Fe, S, P, Na) coming from the extracellular matrix and concentrating and enriching this area. The ESEM analyses of the 12-month implantation bulk samples showed the formation of Ca–P spherical aggregates (Fig. 9). The peculiarity of these new precipitates is that they contain also Fe and Zn: elements that they did not belong to the original material.

The PVC NPs induced granuloma and fibroblastic proliferation at 12 months, whereas the bulk material generated only an inflammatory reaction. Figure 10 shows the PVC aggregated, macrosized particles surrounded by a fibrotic capsule. The EDS investigations in the surrounding tissues identified the additional presence of Ca in the spectrum of PVC.

4 Discussion

Nanoparticles and bulk of the ceramic and polymeric materials induced inflammatory and granulomatose reactions at 12-month post-implantation. Instead, the metallic Ni and Co NPs caused the development of a rhabdomyosarcoma within 6 months and the bulk materials produced only granuloma and preneoplasia at 12 months. The shape seems important in inducing the reaction that seems to be

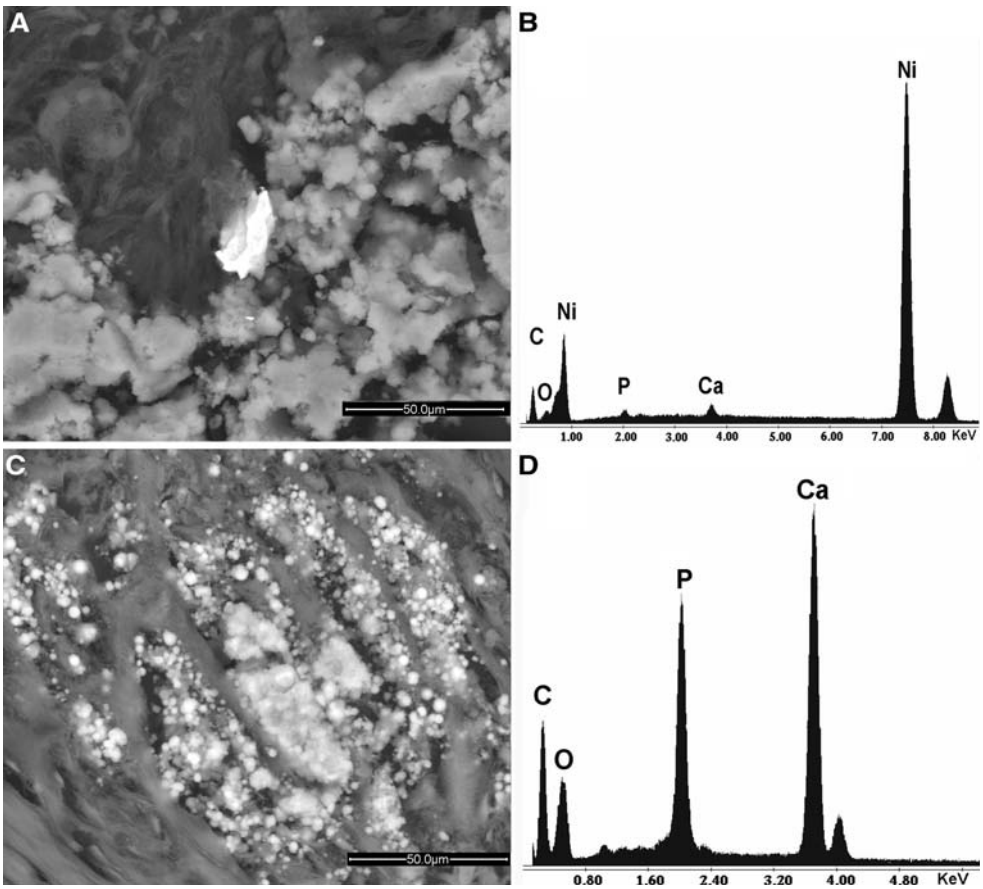

Fig. 4 ESEM images of Ni NP (**a**) and calcium (Ca) and phosphorus (P) spherical particles (**b**) in the area interested by the rhabdomiosarcoma

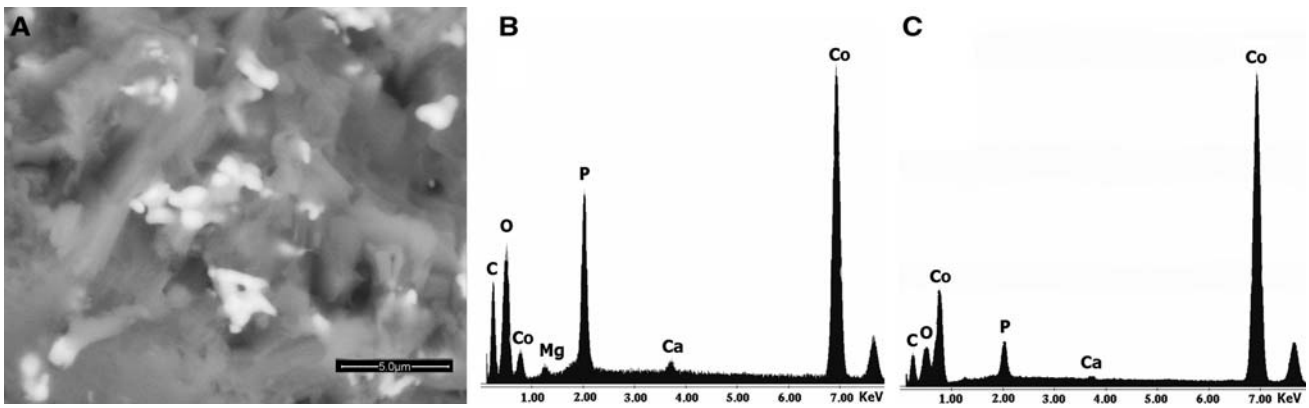

Fig. 5 ESEM image of Co NP implanted in the back of the rat for 6 months with the EDS spectrum. It contains carbon, oxygen, cobalt, phosphorus, calcium and magnesium

delayed in the case of bulk material. A possible explanation could be that the disc of Co may have undergone corrosion or, particularly along the sharp edges of the disc, wear could have occurred due to the micro-movements of the disc itself under the skin, with the ensuing release of sub-micronic particles and ions. These are in a not-equilibrium state, so they recombine immediately (Fig. 6) with proteins or other electrolytes present in the extracellular matrix, forming crystals. In this case, the crystals contain endogenous P, and the diffusion of this element to the implantation area deprived the surrounding tissue of endogenous P. This mechanism could be part of the toxic effect of the metallic debris. The NPs disappear because they are solubilized and transformed into new materials, not biodegradable and of unknown biocompatibility. Interesting is the presence of Mg, S and Ca in the EDS

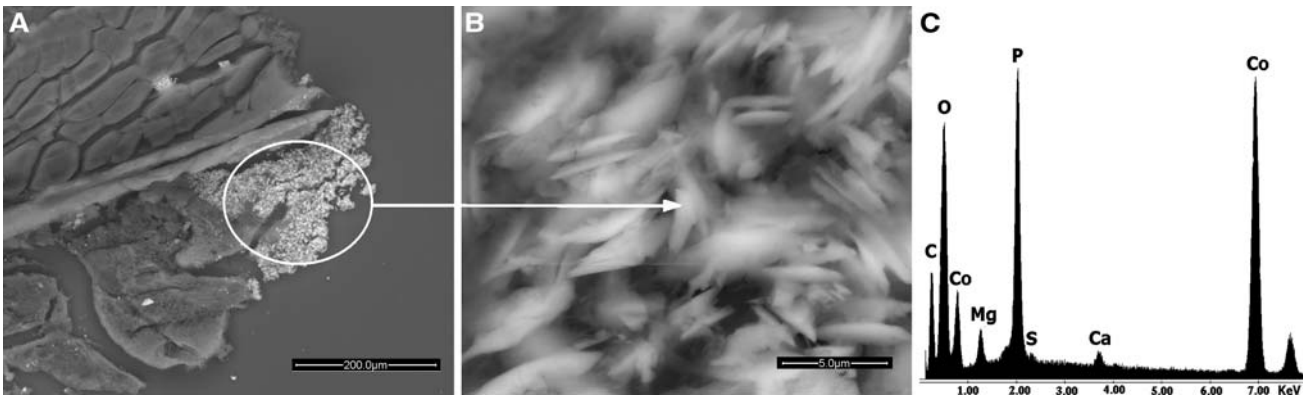

Fig. 6 ESEM image of the 6-month implantation biological reaction of Co NPs in rats (**a**) and Co-P crystals (**b**)

Fig. 7 ESEM image of the area where the silica NPs were implanted. It is rich of calcium–phopshate material containing Silicon

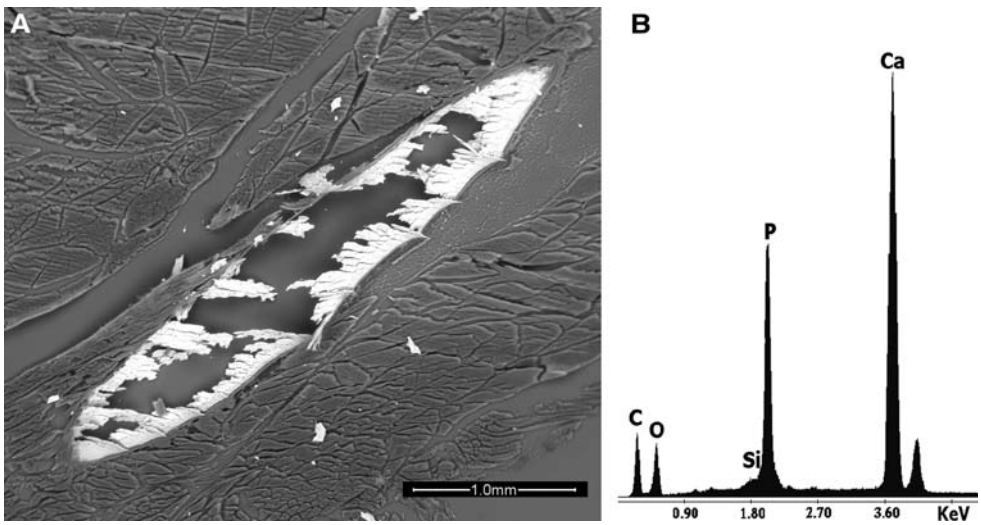

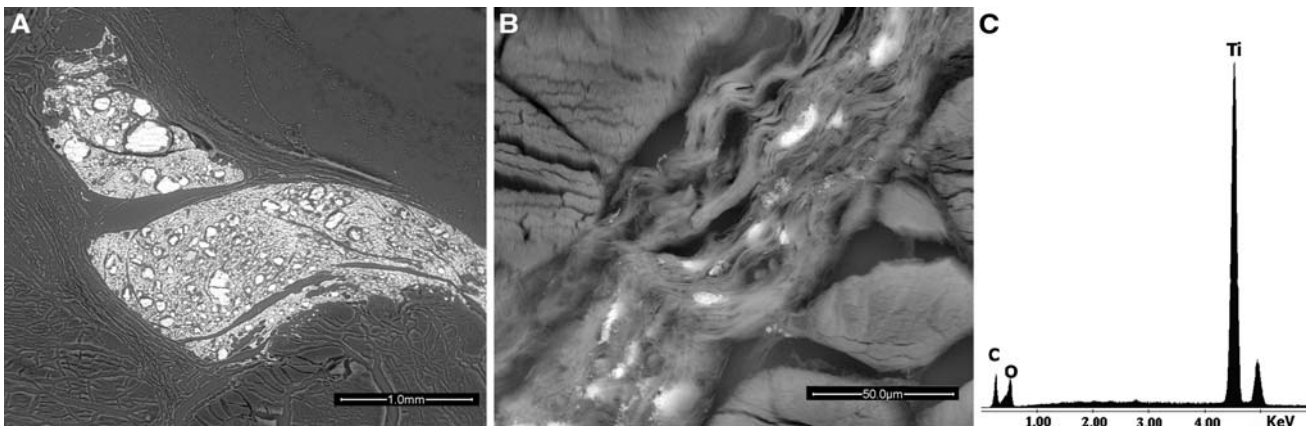

Fig. 8 ESEM images of the area of implantation of titania NPs (**a**) entrapped in a fibrotic tissue (**b**) with the EDS spectrum (**c**)

spectrum. Even if either Ni and Co cause the same pathology, their interactions with the biological matrix is different: Ni gives origin to particles of Ca–P, whereas Co binds to P.

The TiO_2, SiO_2 and PVC NPs after implantation coalesce, forming agglomerates of microscaled size. So, the mild inflammations and granulomas with the formation of fibrous capsules could be considered as a normal "foreign-body" reaction. The wear debris of worn hip joint prostheses induce locally a similar reaction [9, 10]. The transformation of silica NPs into Ca–P is a normal reaction that was already widely analysed when discussing

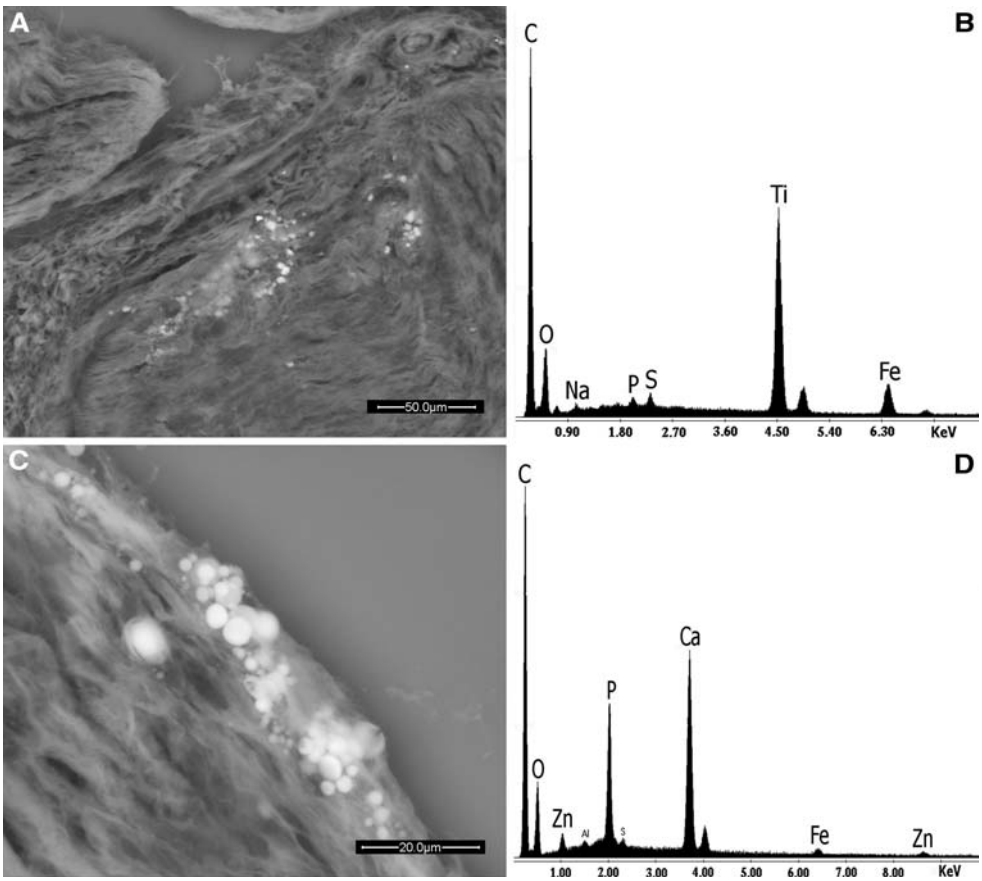

Fig. 9 ESEM image of titania particles after 12-month implantation (**a**) with the EDS spectrum (**b,d**) and the new formed spherical Ca-P particles (**c**)

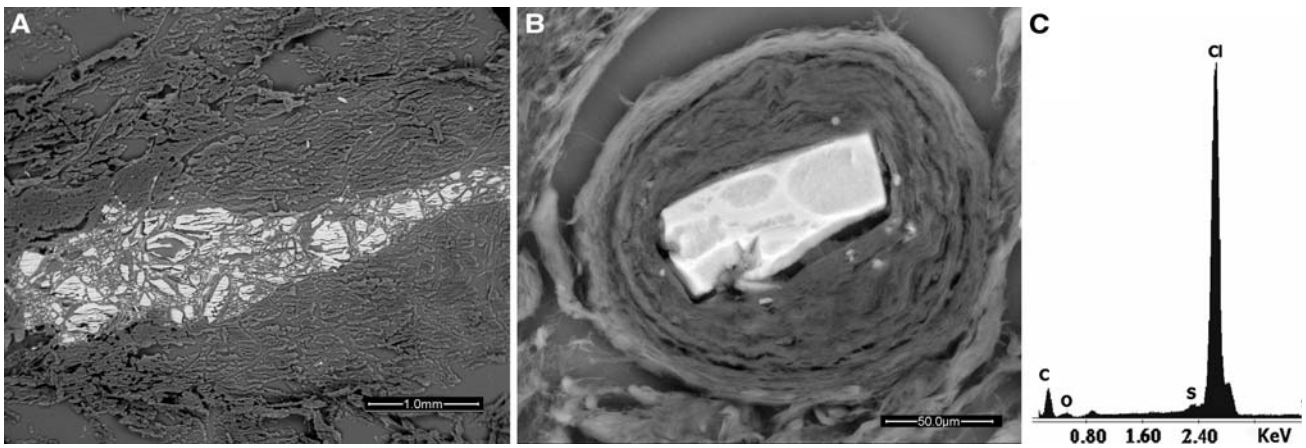

Fig. 10 ESEM image of the area of PVC NP implantation (**a**) with the EDS spectrum (**c**). The image shows a macroscopic particle (due to the coalescence of the NP) surrounded by a capsule of fibrotic tissue (**b**)

bioactive glasses [21, 22]. In that case, there is a transformation in a silica hydrated gel that attracts the Ca and P ions giving origin to a matrix were the osteoblasts can proliferate, forming new bone [23]. The titania NPs induced a different chemical interaction that not only generates an enrichment of Fe, Na, S and P ions close to the titanium particles, but also to spherical presences of Ca–P, containing also Fe and Zn. The formation mechanism of these spherules is not known. PVC did not seem to be prone to chemical interaction: NPs aggregated and induced the classical fibrous capsule. But it must be added that the EDS spectrum identified the presence of Cl in the surrounding tissue: the evidence of a certain degree of dissolution.

5 Conclusions

Size, morphology and chemical composition of exogenous materials are important agents in triggering a pathology. Metallic species seem to induce pathologies with a worse disease course (Ni and Co-induced rhabdomyosarcoma early). What looks of the utmost importance in triggering the pathology is the chemical substrate that is generated by the interaction between tissue and foreign body, which also releases smaller particles and chemicals. The presence of Ca and P precipitates also in spherical shape seems to be part of the evolution of the pathology. It is well known that Ca ions play an important role in the biochemical cascade of signal transduction pathways, leading to the activation of immune cells. So, its sequestration (after precipitation, Ca becomes insoluble and is no longer bioavailable) could activate immunoresponses. P sequestration could prevent the normal synthesis of ADP, ATP, etc., and, as a consequence, alter the normal metabolism.

From these observations, it is clear that biocompatibility studies also need to verify the final state of the exogeous (implanted) materials and their transformations, including induced precipitation of endogenous elements.

Acknowledgements This research was supported by the European Community: project NANOPATHOLOGY, the role of micro and NPs in inducing biomaterial pathologies-QOL-2002-147.

References

1. V.L. Colvin, Nat. Biotechnol. **21**(10), 1166–1170 (2003)
2. A.D. Maynard, R.J. Aitken, T. But, V. Colvin, K. Donaldson, G. Oberdorster, M.A. Philbert, J. Ryan, A. Seaton, V. Stone, S. Tinkle, L. Tran, N.J Walker, D. B. Warheit, Nature **444**(7117), 267–269 (2006)
3. G. Oberdorster, E. Oberdorster, J. Oberdorster, Environ. Health Perspect. **113**, 823–839 (2005)
4. G. Oberdorster, Z. Sharp, V. Atudorei, A. Elder, R. Gelein, A. Lunts, W. Kreyling, C. Cox, J. Toxicol. Environ. Health A, **65**, 1531–1543 (2002)
5. A. Nemmar, P.H. Hoet, B. Vanquickenborne, D. Dinsdale, M. Thomeer, M.F. Hoylaerts, H. Vanbilloen, L. Mortelmans, B. Nemery, Circulation, **105**(4), 411–417 (2002)
6. P.R. Lockman, R.J. Mumper, M.A. Khan, D.D. Allen, Drug Dev. Ind. Pharm. **28**(1), 1 (2002)
7. G. Oberdorster, Z. Sharp, V. Atudorei, A Elder, R. Gelein, W. Kreyling, C. Cox, Inhal. Toxicol. **16**, 437–445 (2004)
8. J.M. Koziara, P.R. Lockman, D.D. Allen, R.J. Mumper, Pharm. Res. **20**(11), 1772 (2003)
9. P.A. Revell, N. Al Saffar, A. Kobayashi, Proc. Inst. Mech. Eng. **211**(H), 187–197 (1997)
10. R. Urban, J. Jacobs, M. Tomlinson, et al., J. Bone Joint Surg. **82A**(4), 455–477 (2000)
11. A.M. Gatti, F. Rivasi, Biomaterials **23**(11), 2381–2387 (2002)
12. A.M. Gatti, Biomaterials **25**(3), 385–392 (2004)
13. A. Nemmar, M.F. Hoylaerts, P.H. Hoet, D. Dinsdale, T. Smith, H. Xu, J. Vermylen, B. Nemery, Am. J. Respir. Crit. Care Med. **166**, 998–1004 (2002)
14. A.M. Gatti, S. Montanari, E. Monari, A. Gambarelli, F. Capitani, B. Parisini, Mater. Sci. Mater. Med. **15**, 469–472 (2004)
15. A.M. Gatti, *Handbook of Nanostructured Biomaterials and their Applications*, vol. 2, (American Scientific Publisher, USA, 2005), pp. 347–369, ch.12
16. S.B. Goodman, V.L. Fornasier, J. Lee, J. Kei, J. Biomed, Mat. Res. **24**, 517–524 (1990)
17. M.C. Pereira M.L. Pereira J.P. Sousa, Biomaterials **20**, 2193–2198 (1999)
18. M. Lucarelli, A.M. Gatti, G. Savarino, P. Quattrini, L. Martinelli, E. Monari, D. Boraschi, Cytokin Network, **15**(4), 1–8 (2004)
19. K. Peters, R. Unger, A.M. Gatti, E. Monari, J. Kirkpatriick, J. Mater. Sci.: Mat. Med. **15**(4), 321–325 (2004)
20. T. Hansen, G. Clermont, A. Alves, R. Eloy, C. Brochhausen, J.P. Boutrand, A. Gatti, J. Kirkpatrick, J. R. Soc.: Interface **3**, 767–775 (2006)
21. A.M. Gatti E. Monari, in *New Biomedical Materials: Basic and Applied Studies*, ed. by P.I. Haris D. Chapman (IOS Press, Amsterdam, 1998), pp. 73–80
22. A.M. Gatti, E. Monari, L. Hench, D. Greenspan, in *Surface Active Processes in Materials*, vol. 101, ed. by D.E. Clark, D.C. Folz, J.H. Simmons (CERAMICS Transactions, Ohio, USA, 2000), pp. 177–184
23. A. Gerth K. Nieber N.J. Oppenheimer S. Hauschildt, Biochem. J. **382**(Pt3), e5–e6 (2004)